

# Numerical Study of Thermal Hydraulic Performance Improvement in Double Pipe Heat Exchangers Using Different Corrugated Tube Geometries

Journal of Mechanical Engineering,  
Science, and Innovation  
e-ISSN: 2776-3536  
2026, Vol. 6, No.1  
DOI: 10.31284/j.jmesi.2026.v6i1.8748  
ejurnal.itats.ac.id/jmesi

Muhammad Hisyam Haidar Al Ghazi<sup>1</sup>, Damora Rhakasywi<sup>1\*</sup>, and Fahrudin<sup>1</sup>

<sup>1</sup> Mechanical Engineering Department, Faculty of Engineering, Universitas Pembangunan Nasional Veteran Jakarta, Indonesia

**Corresponding author:**

*Damora Rhakasywi*

Mechanical Engineering Department, Faculty of Engineering, Universitas Pembangunan Nasional Veteran Jakarta, Indonesia

Email: rhakasywi@upnvj.ac.id

## Abstract

Enhancing thermal efficiency in double-pipe heat exchangers has become a key industrial priority to reduce energy consumption, with passive methods such as pipe geometry modification receiving significant attention. This study investigates the comprehensive thermal and hydraulic performance of concave corrugated tubes (CCT) with triangular, square, and trapezoidal profiles. A three-dimensional numerical simulation was employed, utilizing the finite volume method and the SST  $k-\omega$  turbulence model over a Reynolds number range of 7700 to 13,800. The results indicate that all CCT geometries improve thermal performance compared to plain tubes, with the square profile showing the highest increase in Nusselt number (13.87-16.59%). This enhancement is attributed to higher turbulence intensity, which, however, also results in the greatest hydraulic penalty due to dominant form drag. Performance Evaluation Criteria (PEC) analysis yielded values above 1 for all geometries, with the square profile being optimal at lower Reynolds numbers, whereas the triangular profile outperformed the others at higher flow rates ( $Re > 12,300$ ), with a PEC value of 1.023. In conclusion, corrugated geometries have been shown to enhance thermal performance, but the associated hydraulic penalties necessitate careful selection based on the operational flow range to achieve an optimal balance between heat-transfer gains and pumping-power requirements.

**Keywords:** Double-pipe heat exchanger, heat transfer enhancement, corrugated tube, numerical simulation, performance evaluation criteria.

Received: February 18, 2026; Received in revised: April 8, 2026; Accepted: April 14, 2026

Handling Editor: Hasan Maulana and Safiullah



## **INTRODUCTION**

The growing demand for energy and the increasing global emission footprint have made improving the efficiency of thermal systems a primary priority in the industrial sector [1]. Among the critical components in these systems is the heat exchanger, which plays a vital role in energy conversion and recovery processes across various industrial applications [2]. Heat exchangers are widely used, ranging from household appliances such as air conditioners to complex industrial process equipment [3]. Their applications cover cooling systems, including refrigerators and air conditioners, heating systems, such as water heaters, and dual-function systems, such as those used in oil distillation processes at refineries [4],[5]. In modern industry, heat exchanger design is increasingly focused on achieving high thermal performance by minimizing heat loss to the environment and reducing pressure drop, thereby lowering required pump power and operational costs [6].

Among the various types of heat exchangers, the double pipe heat exchanger (DPHE) is one of the simplest and remains widely used, especially in high-pressure and medium-scale industrial applications, due to its resistance to pressure, ease of maintenance, and relatively low fabrication costs compared to other types [7],[8]. The DPHE has a straightforward construction, consisting of two concentric pipes, with hot and cold fluids flowing separately in the inner pipe and the annular space, where the inner pipe wall serves as the heat transfer medium [9]. Despite its advantages, the conventional DPHE is limited by a relatively low heat transfer coefficient compared to other types of heat exchangers [10]. This limitation often requires a longer unit to achieve the desired heat transfer load, resulting in inefficiencies in both space and material utilization [11].

To address these limitations, previous studies aimed at enhancing heat transfer in double pipe heat exchangers (DPHE) have predominantly employed passive methods that require no additional external power. Passive heat transfer enhancement techniques in DPHEs are generally classified into three main categories: pipe geometry modification, the addition of flow-disturbing elements such as turbulators or swirl generators, and the use of fluid additives, such as nanofluids, to improve thermal performance without additional energy input [12],[13]. In contrast, pipe geometry modification may involve adding fins to the pipe wall or transforming the pipe into a corrugated tube, both of which can enhance thermal performance by increasing local turbulence and expanding the heat transfer area [14].

Corrugating pipe geometry is a widely used passive method that primarily boosts DPHE thermal performance by enhancing mixing and convective heat transfer through induced flow disturbances. It also remains simple to manufacture [15]. However, while corrugated tubes enhance heat transfer, they also increase pressure drop and friction factor; therefore, both thermal and hydraulic aspects must be evaluated simultaneously. The thermal-hydraulic performance of corrugated pipes strongly depends on corrugation geometry, including profile, depth, and pitch, which govern flow disturbance. Therefore, selecting an appropriate configuration requires balancing both thermal enhancement and hydraulic penalty [16]. These tubes can be configured as concave or convex profiles and applied to either the inner or outer pipe[15].

For example, the use of spirally inner corrugated tubes under turbulent flow with variations in pitch and corrugation height demonstrated that the configuration with the smallest pitch and moderate height increased NTU by up to 29% compared to smooth tubes, while the configuration with the largest corrugation height increased the inner-side pressure drop by up to 4.15 times [17]. This indicates a clear trade-off between heat transfer enhancement and hydraulic penalty, where aggressive geometric modifications tend to significantly increase friction losses. The application of corrugated fins to the inner pipe of coaxial underground heat exchangers (CUHEs) has also been shown to significantly enhance heat transfer, with the Nusselt number 1.43-2.19 times higher than

that of smooth pipes. However, this improvement is accompanied by a 6.79-fold increase in the friction factor. Although an optimal configuration (fin width of 15 mm and spacing of 60 mm) achieved a maximum PEC of 1.34 at  $Re = 12,000$ , the study remains limited to a specific fin geometry and does not explore the influence of different corrugation shapes on the thermal-hydraulic balance [16].

Other studies using externally corrugated inner tubes (ECIT) and internally corrugated inner tubes (ICIT) in DPHEs with water,  $SiO_2$ , or CuO nanofluids in the Reynolds number range of 4,000 to 20,000 have demonstrated that the ECIT configuration with a 15-degree helix angle provides the highest Performance Evaluation Criteria (PEC), and the use of CuO nanofluid can increase the Nusselt number by up to 35 percent with PEC values between 0.89 and 2.09 [18]. Despite these improvements, the combined effects of fluid properties and geometric modification make it difficult to isolate the sole contribution of corrugation geometry to performance enhancement. In boiling R290 refrigerant flow, the use of internal corrugated tubes with square and circular profiles yielded heat transfer enhancement factors (E1) of 2.01-2.36 (square) and 1.67-1.98 (circular), with efficiency indices (I) above 1 (1.05-1.24 and 1.13-1.29), indicating significant heat transfer improvement with pressure penalties that remain acceptable [19]. However, these studies are limited to phase-change conditions and do not directly reflect single-phase turbulent flow behavior in conventional DPHE applications.

Studies focusing on corrugated outer pipes with smooth inner tubes showed that reducing pitch and diameter ratio can increase the Nusselt number by up to 71%. This improvement is accompanied by an 81% increase in the friction factor [20]. Outward helically corrugated tubes revealed that reducing the shell diameter enhances both heat transfer and pressure drop. An optimal diameter of 38 mm was suggested as a compromise [21]. These findings highlight the strong influence of geometric modifications on heat exchanger performance; however, most studies focus on parametric variations within a single corrugation type rather than comparing different geometries, and offer limited discussion of the underlying flow mechanisms. The use of concave corrugated tubes in the inner pipe of DPHEs with three groove shapes (triangular, trapezoidal, and square) has been shown to improve heat transfer characteristics, with the triangular groove yielding an effectiveness increase of up to 11.63% over plain tubes [22]. While the study primarily focuses on thermal performance, it does not offer a comprehensive evaluation of friction factor, pressure drop, or overall performance (PEC).

This study uniquely addresses the identified research gap by systematically comparing concave corrugation geometries (triangular, square, and trapezoidal) applied to the inner tube of a double pipe heat exchanger under identical operating conditions. Unlike previous work, this research exclusively isolates the effect of corrugation shape on thermal-hydraulic performance in single-phase turbulent flow, an area that has not been comprehensively explored. The study integrates flow-field analysis (velocity and turbulent kinetic energy) with thermal and hydraulic evaluations, and uses Performance Evaluation Criteria (PEC) to assess the trade-off between heat transfer enhancement and pressure drop. By clarifying the specific impact of corrugation geometry, this work lays a new foundation for optimizing heat exchanger design.

## **METHODS AND ANALYSIS**

### **Physical Model**

The computational domain for the double pipe heat exchanger (DPHE) with a concave corrugated tube is shown in Figure 1. Water is used as the working fluid on both the hot and cold sides, with a counterflow arrangement: hot fluid passes through the inner pipe, and cold fluid flows in the annulus between the pipes. Key dimensions include an inner pipe diameter of 25.4 mm, outer pipe diameter of 76.2 mm, total length of 1000 mm,

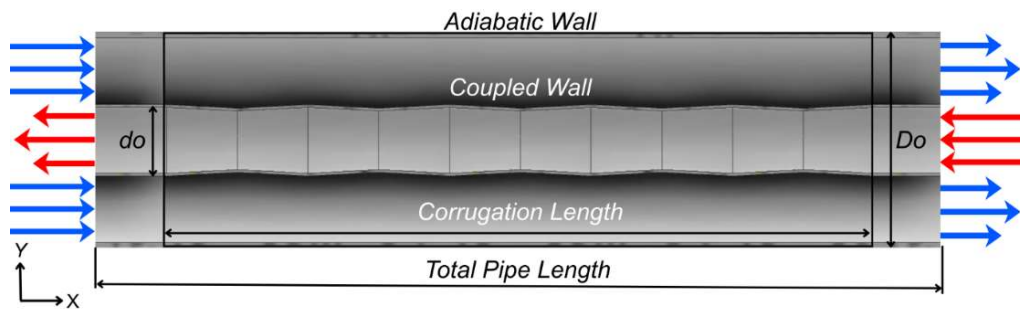


**Figure 1.** Computational domain schematic of the DPHE

**Table 1.** Dimensional details of the DPHE

Dimensions	Outer Pipe (mm)	Inner Pipe (mm)
Outer Diameter ( $Do, do$ )	76.2	25.4
Inner Diameter ( $Di, di$ )	72.6	23.4
Thickness ( $to, ti$ )	2	1
Length ( $L$ )	1000	1000
Corrugation Length ( $Lc$ )	-	850

and a corrugated section length of 850 mm, as detailed in Table 1. These specifications follow previous research [22] on the heat transfer effectiveness of different concave corrugated tube geometries.

### Boundary Conditions And Numerical Methods

The boundary conditions specified in the numerical modeling of the DPHE are as follows. The inlet is defined as a mass flow inlet. The mass flow rate ( $\dot{m}h$ ) ranges from 0.05 to 0.09 kg/s, with a constant temperature ( $T_h$ ) of 353.15 K and a hydraulic diameter ( $D_h$ ) of 0.0234 m for the inner pipe. For the annulus, the mass flow rate ( $\dot{m}c$ ) is set at 0.1 kg/s. The temperature ( $T_c$ ) is held constant at 303.15 K, and the hydraulic diameter ( $D_c$ ) is 0.0478 m. A turbulence intensity of 5% is applied at both inlets. The outlets for both the inner pipe and the annulus are defined as pressure outlets with a gauge pressure of 0 Pa and a turbulence intensity of 5%. The outer pipe wall is modeled as an adiabatic wall, while the inner pipe wall is defined as a coupled wall with a no-slip boundary condition. Detailed boundary conditions used in this study are presented in Table 2.

The materials used in this numerical modeling are stainless steel 304 for the outer pipe and copper for the inner pipe. The material properties, including density ( $\rho$ ), specific heat capacity ( $C_p$ ), and thermal conductivity ( $k$ ), are listed in Table 3. For the working fluid, due to the substantial temperature difference between the inlet and outlet, which ranges from 303.15 K to 353.15 K as shown in Table 4, the properties of water, including density ( $\rho$ ), specific heat capacity ( $C_p$ ), thermal conductivity ( $\lambda$ ), and viscosity ( $\mu$ ), are defined as temperature-dependent values. These properties are determined using a piecewise linear function based on steam tables.

**Table 2.** Boundary conditions of DPHE

Boundary Conditions	Type	Input	
Inlet	Mass flow inlet	$\dot{m}h = 0.05-0.09$ kg/s	$\dot{m}c = 0.1$ kg/s
		$T_h = 353.15$ K	$T_c = 303.15$ K
		$D_h = 0.0234$ m	$D_c = 0.0478$ m
		Turbulent intensity = 5%	
Outlet	Pressure outlet	Pressure gauge = 0 Pa	Turbulent Intensity = 5%
Inner Pipe	Coupled wall	No-slip boundary condition	
Outer Pipe	Adiabatic wall	Heat flux = 0	

**Table 3.** Material properties of DPHE

Material Properties	Stainless Steel 304	Copper
Density ( $\rho$ ) (Kg/m <sup>3</sup> )	8000	8978
Specific heat capacity ( $C_p$ ) (J/Kg.K)	500	381
Thermal conductivity ( $k$ ) (W/m.K)	16.2	387.6

**Table 4.** Properties of water based on temperature

Temperature (K)	$\rho$ (Kg/m <sup>3</sup> )	$C_p$ (J/Kg.K)	$\lambda$ (W/m.K)	$\mu$ (Pa.s)
303.15	995.8	4178	0.6151	0.0007977
353.15	971.4	4196	0.6668	0.00355

Numerical simulations using the SST  $k-\omega$  model were conducted at  $Re = 7,700-13,800$ , ensuring accurate prediction of near-wall flow and separation [23]. Mesh quality maintained  $y^+ \leq 1$ , while radiative heat transfer was neglected. A coupled algorithm with second-order upwind schemes was applied, with convergence criteria of  $10^{-6}$  for the energy equation and  $10^{-4}$  for the continuity, momentum, and turbulence equations.

### Grid Generation and Verification

Grid generation employed hexahedral and tetrahedral elements, which are well-suited for the complex geometry of concave corrugated tubes. Figure 2 shows the detailed grid structure of the DPHE. Due to complex flow behavior, mesh refinement was applied near the wall and in the corrugated regions, with a target  $y^+ \leq 1$ , suited to the SST  $k-\omega$  model. Grid quality was maintained with skewness  $< 0.94$  to ensure numerical accuracy.

Grid verification was conducted using the Grid Convergence Index (GCI) method proposed by Roache [24] to ensure the numerical solution's independence from grid density. The test was performed on the DPHE with triangular CCT variation at  $Re = 10,700$ , using grid densities of  $1.2 \times 10^6$  (coarse),  $1.8 \times 10^6$  (medium), and  $2.9 \times 10^6$  (fine). The observed parameters were the outlet temperature ( $T_{out}$ ) and the pressure drop ( $\Delta P$ ) of the hot fluid, as shown in Table 5.

Based on the grid verification using the GCI Roache method, as presented in Table 5, the ratio of  $\frac{GCI_{fine}}{r^p GCI_{coarse}}$  is approximately one, indicating that the solution lies within the asymptotic range and the grid can be considered convergent. The medium grid was selected for this study because the  $GCI_{fine}$  values for both  $T_{out}$  and  $\Delta P$  are very small, providing a solution that is sufficiently independent of the grid.

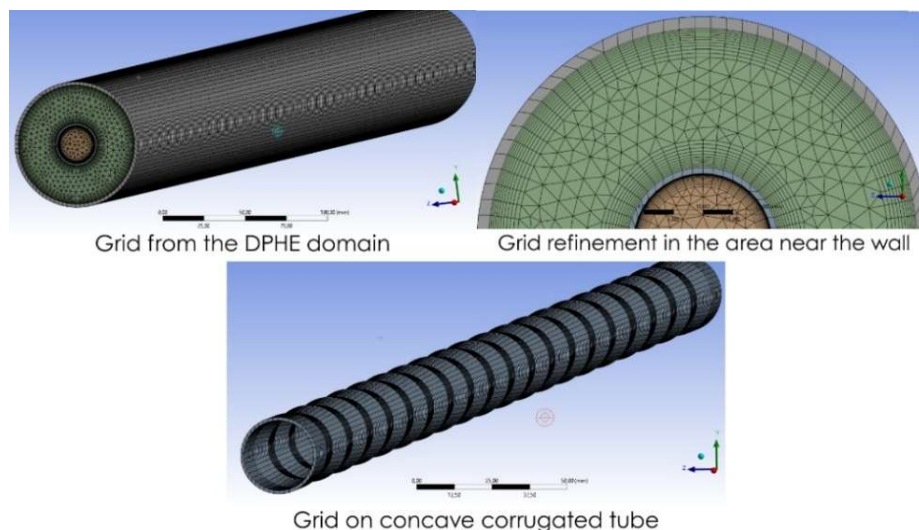


**Figure 2.** Grid details from DPHE

**Table 5.** Grid verification using the GCI method

Grid	Th <sub>out</sub> (K)	r	p	GCI (%)	$\frac{GCI_{fine}}{r^p GCI_{coarse}}$	Error (%)	ΔP (Pa)	p	GCI (%)	$\frac{GCI_{fine}}{r^p GCI_{coarse}}$	Error (%)
Fine	349.13			0.02		-	27.85		1.46		-
Medium	349.11	1.16	3.4	0.04	1.00	0.01	27.99	2.33	2.05	1.00	0.48
Coarse	349.14			-		0.01	28.18		-		0.68

### Data Acquisition and Analysis

To evaluate the impact of using concave corrugated tubes on the thermal and hydraulic performance of the DPHE, this study employs the Nusselt number (Nu), friction factor (f), and performance evaluation criterion (PEC) as performance indicators. The definitions and calculation methods for these parameters form the basis for the subsequent analysis of the numerical simulation results [14],[19].

Nu is defined as Eq.1. Where λ is the thermal conductivity of the fluid, D is the hydraulic diameter of the DPHE, and h is the heat transfer coefficient obtained from Eq.2:

$$Nu = \frac{hD}{\lambda} \tag{1}$$

$$h = \frac{q}{T_w - T_f} \tag{2}$$

Where q is the heat flux on the inner side of the inner pipe, T<sub>w</sub> is the temperature on the inner side of the inner pipe, and T<sub>f</sub> is the average temperature of the fluid obtained from Eq.3:

$$T_f = \frac{Th_{in} + Th_{out}}{2} \tag{3}$$

Where Th<sub>in</sub> and Th<sub>out</sub> are the fluid temperatures at the inlet and outlet of the DPHE. The friction factor is expressed as Eq.4:

$$f = \frac{2D\Delta P}{L\rho u^2} \tag{4}$$

Where ΔP is the pressure difference at the inlet and outlet, L is the length of the DPHE, ρ is the fluid density, and u is the average flow rate.

PEC is formulated as Eq.5:

$$PEC = \frac{Nu/Nu_s}{(f/f_s)^{1/3}} \tag{5}$$

Where Nu<sub>s</sub> and f<sub>s</sub> are Nu and f from DPHE with a smooth inner pipe at the same Re.

### Model Validation

To ensure the accuracy of the numerical modeling, validation was performed by comparing the simulated Nusselt number (Nu) values for the DPHE with plain tubes against the Dittus-Boelter [25] and Gnielinski [26] correlations. Similarly, the simulated friction factor (f) values for the DPHE with plain tubes were compared with the Blasius [27] and Petukhov [28] correlations.

Dittus-Boelter Correlation (Eq.6):

$$Nu = 0.023Re^{0.8}Pr^{0.3} \tag{6}$$

With a range of applications  $10^4 \leq Re \leq 1.2 \cdot 10^5$  and  $0.7 \leq Pr \leq 120$ .

Gnielinski's correlation (Eq.7):

$$Nu = \frac{(f/8)(Re - 1000)Pr}{1 + 12.7(f/8)^{1/2} (Pr^{2/3} - 1)} \quad (7)$$

With a range of applications  $3000 \leq Re \leq 10^6$  and  $0.5 \leq Pr \leq 2000$ .

Blasius correlation (Eq.8):

$$f = 0.316Re^{-0.25} \quad (8)$$

With a range of applications  $4000 \leq Re \leq 10^5$ .

Petukhov's correlation (Eq.9):

$$f = (0.79 \ln Re - 1.64)^{-2} \quad (9)$$

With a range of applications  $3000 \leq Re \leq 10^6$ .

The Reynolds number for the fluid in the inner pipe was calculated using the following equation Eq.10:

$$Re = \frac{4\dot{m}}{\pi d_i \mu} \quad (10)$$

Where  $\dot{m}$  is the mass flow rate,  $\mu$  is the fluid viscosity, and  $d_i$  is the inner pipe diameter.

The Reynolds number for the fluid in the annulus was calculated using the following equation (Eq.11):

$$Re = \frac{4\dot{m}}{\pi(D_i + d_o)\mu} \quad (11)$$

Where  $D_i$  is the inner diameter of the outer pipe and  $d_o$  is the outer diameter of the inner pipe.

As shown in Figure 3, the average absolute deviation of the simulated Nusselt number (Nu) (Green) is 1.26% compared to the Dittus-Boelter correlation (purple) and 7.38% compared to the Gnielinski correlation (orange). For the friction factor (f) (blue), the deviations are 6.29% and 6.75% compared to the Blasius (red) and Petukhov correlations (light green), respectively. These results show good agreement between the numerical model and the empirical correlations, validating the model.

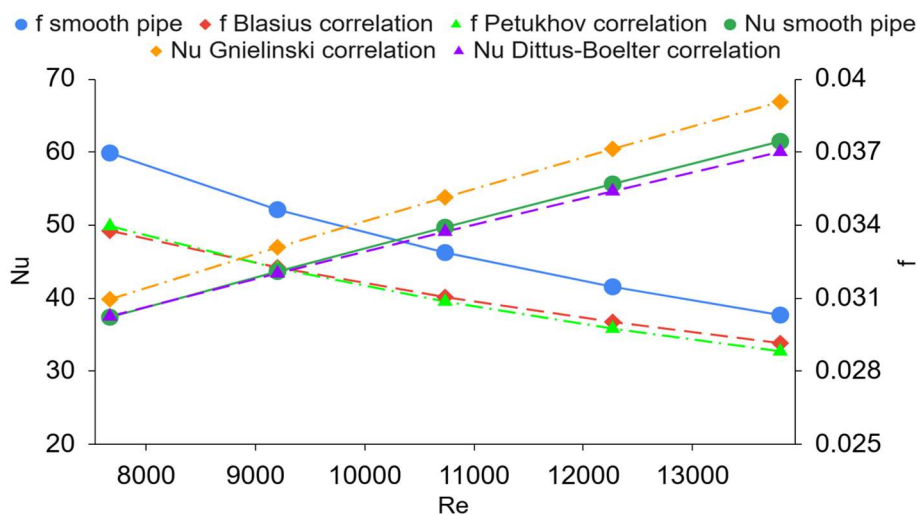


**Figure 3.** Numerical validation of Nu and f from DPHE with smooth inner pipe

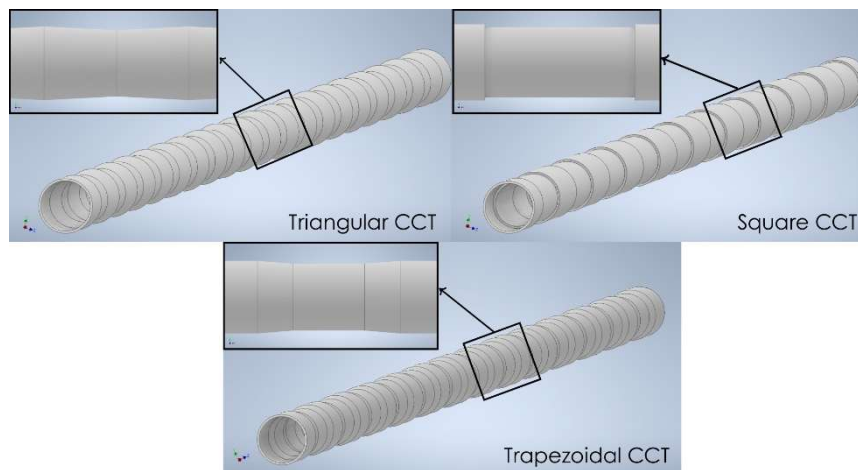


**Figure 4.** Details of the concave corrugated tube geometries

### **Concave Corrugated Tube Geometry**

The three concave corrugated tube (CCT) geometries compared in this study are triangular, square, and trapezoidal, each with a corrugation height of 1 mm, as shown in Figure 4. The detailed dimensions are as follows: for the triangular geometry, both the corrugation length and pitch are 50 mm; for the square geometry, the corrugation length is 50 mm, and the pitch is 100 mm; and for the trapezoidal geometry, the corrugation length is 50 mm, the pitch is 75 mm, and the short side length is 25 mm. The corrugated section is 850 mm long, accounting for 85% of the inner pipe's total length.

## **RESULTS AND DISCUSSIONS**

### **Flow Field Characteristics**

The velocity and turbulent kinetic energy (TKE) contour visualizations in Figures 5 and 6 reveal clear differences in flow characteristics among the CCT geometries. All models exhibit a high-velocity core at the channel center, with velocity decreasing toward the wall due to viscous effects. In the triangular CCT, flow disturbances and increased TKE are concentrated around sharp corners, indicating local vortex formation and intensified shear layers. The square profile shows broader recirculation zones and more extensive TKE regions, indicating stronger turbulence and greater flow separation. In contrast, the trapezoidal profile produces smoother velocity gradients and a more uniform TKE distribution, resulting in weaker disturbances. These findings suggest that sharper corrugation transitions, as found in the square CCT, more effectively disrupt the boundary layer and enhance turbulence generation, which is consistent with previous studies reporting higher heat transfer enhancement with stronger flow disturbance [17]. This behavior highlights the direct correlation between turbulence intensity and convective heat transfer enhancement in corrugated geometries. Therefore, the square CCT profile generates the most significant turbulence and offers the highest potential for Nusselt number enhancement, whereas the trapezoidal profile yields the lowest thermal performance improvement.

### **Temperature Distribution**

The temperature contour visualizations in Figure 7 show how different concave corrugated tube (CCT) geometries affect temperature distribution and thermal boundary layer thickness near the pipe wall. All geometries maintain a high-temperature core at the channel center. A sharp temperature gradient develops toward the wall. In areas with high turbulent kinetic energy (TKE), localized thinning of the thermal boundary layer is observed, depending on the profile shape. For the square profile, expanded high-TKE zones correlate with significant boundary-layer thinning. These areas also show higher wall-temperature gradients and enhanced surface heat flux. The triangular profile causes

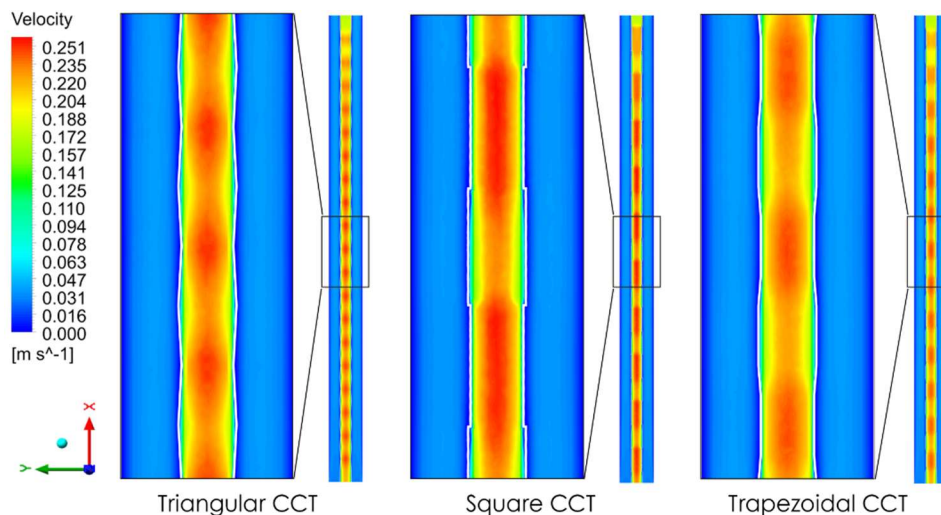


**Figure 5.** Velocity contours from DPHE with CCT at  $Re \approx 10700$

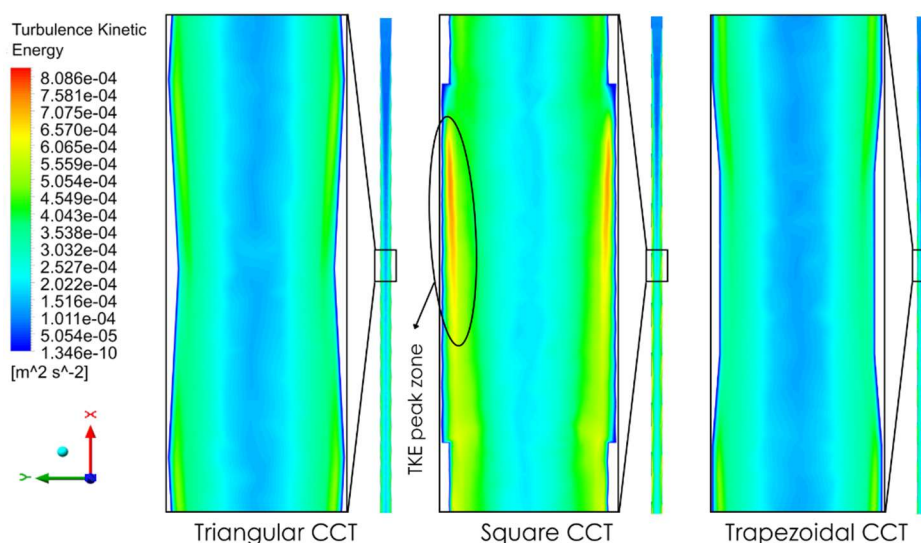


**Figure 6.** Contour of turbulent kinetic energy (TKE) from DPHE with CCT at  $Re \approx 10700$

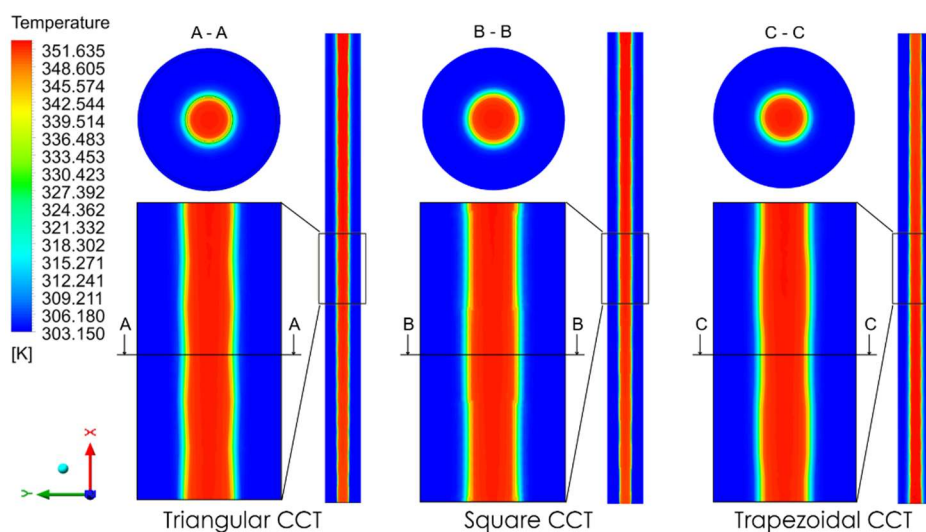


**Figure 7.** Temperature contours of DPHE with CCT at  $Re \approx 10700$

localized thinning at sharp corners and noticeable temperature fluctuations. The trapezoidal profile produces a more uniform temperature field with a thicker boundary layer, suggesting weaker disturbances. These results demonstrate that increased turbulence and boundary-layer disruption, especially in the square profile, enhance

mixing and reduce wall thermal resistance, consistent with previous studies on corrugated tubes reporting enhanced heat transfer due to intensified turbulence [22]. This agreement reinforces the role of flow-induced mixing as a dominant mechanism governing thermal performance in corrugated geometries.

### Thermal Performance Evaluation

Figure 8 compares Nusselt numbers (Nu) for the plain tube and three CCT geometries over a Reynolds number (Re) range of 7700-13,800. All CCT geometries yield higher Nu values than the plain tube. This confirms that wall modification enhances convective heat transfer. The square profile shows the greatest improvement (13.87-16.59%), followed by the triangular (9.48-10.51%) and trapezoidal (7.21-8.80%) profiles. This trend aligns with earlier flow-field analysis. That analysis showed that the square geometry produced the strongest flow disturbances and the most intense mixing near the boundary layer. These enhancements arise from stronger boundary-layer disruption and turbulence in sharper corrugation transitions, particularly in the square profile, promoting boundary-layer renewal and higher wall-temperature gradients, consistent with previous studies reporting increased Nu due to enhanced mixing [20]. The graph further shows that Nu for all variations increases with Re. However, the rate of improvement is greatest for the square profile at higher Re, while the triangular and trapezoidal profiles show diminishing enhancement. These findings highlight the importance of geometric optimization for maximizing heat exchanger performance, especially in turbulent flow. These results indicate that at higher turbulence levels, the square profile provides the greatest thermal advantage.

### Pressure Distribution

The static pressure distribution within the fluid domain for the three CCT geometries is shown in Figure 9. In general, pressure decreases consistently along the channel. However, the concave wall modifications induce local pressure fluctuations due to repeated flow expansion and contraction. The square CCT profile exhibits the steepest pressure gradients at the corrugation corners. This contrasts with the triangular and trapezoidal profiles. The sharper gradients indicate greater form drag from abrupt changes in flow direction caused by the perpendicular angles. These abrupt changes amplify velocity gradients and intensify boundary layer separation. This leads to stronger recirculation and higher energy dissipation. Such phenomena are closely associated with extensive recirculation and turbulence-induced kinetic energy dissipation in the square profile. Increased turbulence and boundary-layer disruption enhance heat transfer but also increase pressure drop. This is consistent with previous studies reporting higher pressure drops in corrugated tubes due to more intense flow disturbances [19]. The trapezoidal profile demonstrates a more uniform pressure distribution. Its sloped geo-

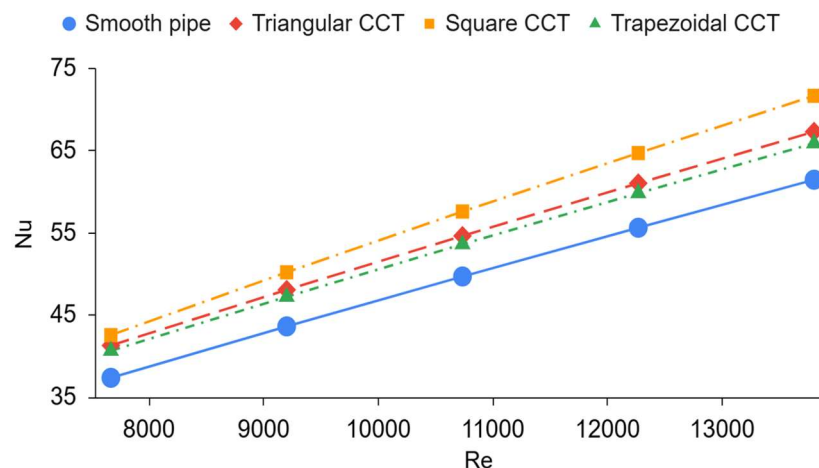
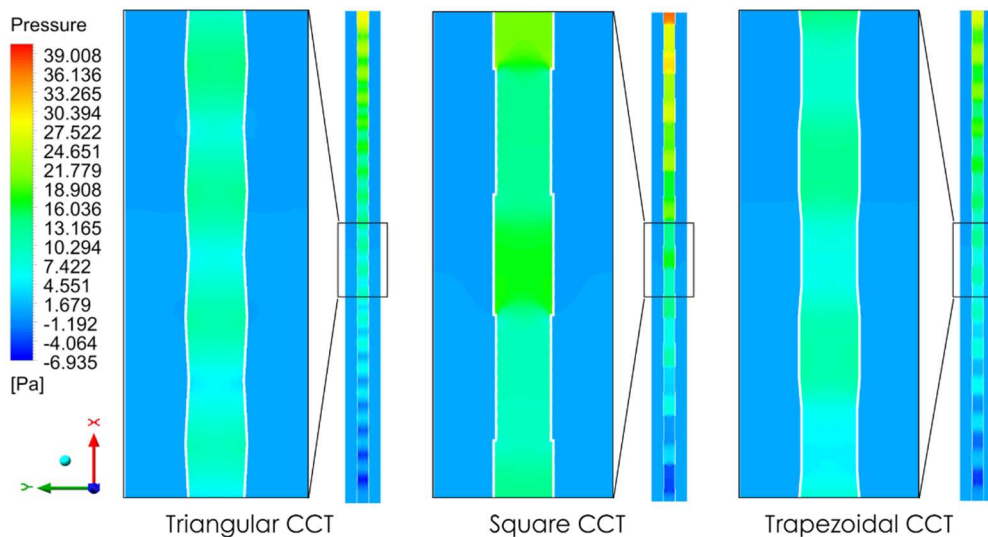
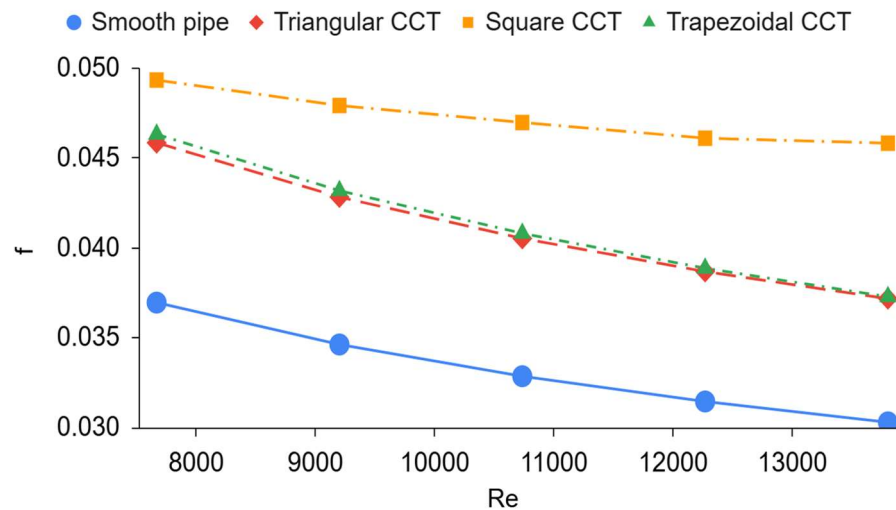


Figure 8. Graph of Nu values from DPHE with CCT variation against Re



**Figure 9.** Static pressure contour of DPHE with CCT at  $Re \approx 10700$



**Figure 10.** Graph of  $f$  values from DPHE with CCT variation against  $Re$

metry helps minimize severe flow separation. These characteristics show that geometries causing the strongest flow disturbances result in the greatest pressure drop.

### Hydraulic Performance Evaluation

The evaluation of hydraulic performance in this study is presented in terms of the relationship between the friction factor and Reynolds number over the range of 7700 to 13,800, as shown in Figure 10. In general, both the plain tube and the three-concave corrugated tube (CCT) geometries exhibit a decreasing trend in friction factor with increasing Reynolds number, consistent with turbulent flow in closed channels. Nevertheless, applying geometric modifications to the tube wall results in a significant increase in the friction factor compared to the plain tube.

Among the three tested geometries, the square CCT profile consistently produces the highest friction factor across the entire Reynolds number range. This sharp increase closely correlates with previous flow-field observations, where perpendicular angles promote extensive recirculation zones and high kinetic-energy dissipation due to dominant form drag. Physically, sharper transitions and abrupt angles in the square CCT intensify turbulence and boundary-layer separation, increasing energy dissipation and wall shear stress, consistent with previous studies reporting higher hydraulic losses in corrugated heat exchangers due to intensified flow disturbances [21]. Meanwhile, the trapezoidal and triangular profiles exhibit lower friction factors, with similar trends at higher Reynolds numbers, indicating more aerodynamic transitions and lower hydraulic

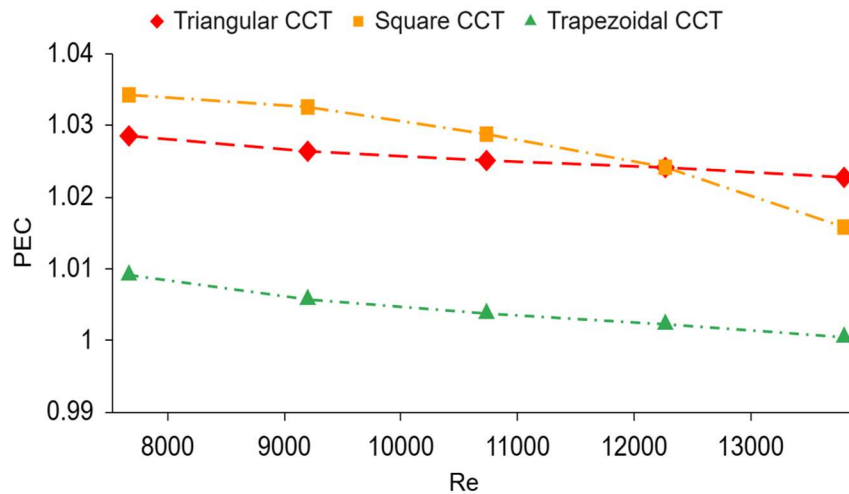


**Figure 11.** Graph of PEC values from DPHE with CCT variation against Re

penalties. Thus, while CCTs enhance heat transfer through turbulence and boundary-layer renewal, they also increase pressure losses, requiring higher pumping power.

### Overall Performance Evaluation

The simultaneous evaluation of thermal and hydraulic performance was conducted using the Performance Evaluation Criteria (PEC) parameter to determine the optimal geometry. Figure 11 shows that PEC values for all concave corrugated tube (CCT) variations remain above unity across the tested Reynolds number range. This indicates that heat transfer enhancement outweighs the associated pressure loss. PEC values for all three geometries generally decrease with increasing Reynolds number. This suggests the effectiveness of passive modification is more pronounced at lower flow velocities. Previous studies on corrugated tubes also report that PEC decreases at higher Re due to dominant hydraulic penalties [18].

At low Reynolds numbers ( $Re \approx 7700$ ), the square CCT profile attains the highest PEC value, followed by the triangular and trapezoidal profiles. The square profile's high PEC stems from a dominant increase in the Nusselt number relative to the friction factor. Intensified turbulence and boundary layer disruption at lower Re promote convective heat transfer more than the increase in hydraulic resistance. This local turbulence enhances mixing and increases the wall temperature gradient. It maximizes heat transfer at low flow rates. As the Reynolds number increases, the square profile's PEC declines. Beyond  $Re \approx 12,300$ , the triangular profile becomes more optimal. At higher Re ( $\approx 13,800$ ), the triangular profile achieves the highest PEC, while the square profile drops further. At high Re, hydraulic penalties for the square profile outweigh heat transfer gains, shifting the efficiency advantage to the triangular geometry. The triangular design achieves a more favorable balance between mixing enhancement and pressure loss under turbulent flow. These trends are consistent with findings in prior corrugated heat exchanger studies [18]. The trapezoidal profile consistently yields the lowest PEC values, as its thermal improvement is least pronounced.

### CONCLUSIONS

In summary, this study provides a comprehensive numerical assessment of the impact of concave corrugated tube (CCT) geometries on the thermal-hydraulic performance of double-pipe heat exchangers. All tested CCT geometries significantly enhance convective thermal performance compared to plain tubes, with Performance Evaluation Criteria (PEC) values consistently above 1. The square profile yields the largest increase in the Nusselt number (13.87% to 16.59%) due to extensive recirculation zones and strong turbulence near the pipe wall, but this improvement is accompanied by a

substantial hydraulic penalty from increased friction caused by form drag at perpendicular corners. While the square profile is most effective at lower Reynolds numbers ( $Re \approx 7700$ ,  $PEC 1.034$ ), the triangular profile becomes more optimal at higher velocities ( $Re \approx 13,800$ ,  $PEC 1.023$ ), providing a better balance between heat transfer and pressure loss. These results underscore the importance of selecting the appropriate corrugation geometry according to specific operating conditions to maximize energy efficiency. For future research, optimization of the corrugation pitch and the use of nanofluids are recommended to further enhance the performance of double-pipe heat exchangers.

#### DECLARATION OF CONFLICTING INTERESTS

The authors declare that they have no potential conflicts of interest regarding the research, authorship, and/or publication of this article.

#### FUNDING

The author(s) disclosed receipt of financial support for the research, authorship, and/or publication of this article.

#### REFERENCES

- [1] S. Sundaramoorthy, D. Kamath, S. Nimbalkar, et al., "Energy Efficiency as a Foundational Technology Pillar for Industrial Decarbonization," *Sustain.*, vol. 15, no. 12, pp. 1-24, 2023, doi: 10.3390/su15129487.
- [2] D. Brough, J. Ramos, B. Delpech, et al., "Development and validation of a TRNSYS type to simulate heat pipe heat exchangers in transient applications of waste heat recovery," *Int. J. Thermofluids*, vol. 9, pp. 1-23, 2021, doi: <https://doi.org/10.1016/j.ijft.2020.100056>.
- [3] S. Ghani, S. M. A. Gamaledin, M. M. Rashwan, et al., "Experimental investigation of double-pipe heat exchangers in air conditioning applications," *Energy Build.*, vol. 158, pp. 801-811, 2018, doi: 10.1016/j.enbuild.2017.10.051.
- [4] B. Abdulmumuni, A. M. Ayoade, O. O. Buhari, et al., "Design, Fabrication and Performance Evaluation of a Shell and Tube Heat Exchanger for Practical Application," *Eur. J. Eng. Res. Sci.*, vol. 5, no. 8, pp. 835-845, 2020, doi: 10.24018/ejers.2020.5.8.1997.
- [5] D. Chavan, P. Joshi, S. Wankhede, et al., "Experimentation on Fabrication of Double Pipe Heat Exchanger," *Int. J. Res. Appl. Sci. Eng. Technol.*, vol. 11, no. 4, pp. 2659-2667, 2023, doi: 10.22214/ijraset.2023.50728.
- [6] O. Arsenyeva, L. Tovazhnyanskyy, P. Kapustenko, et al., "Review of Developments in Plate Heat Exchanger Heat Transfer Enhancement for Single-Phase Applications in Process Industries," *Energies*, vol. 16, no. 13, pp. 1-28, 2023, doi: 10.3390/en16134976.
- [7] H. M. Maghrabie, K. Elsaid, A. T. Sayed et al., "Intensification of heat exchanger performance utilizing nanofluids," *Int. J. Thermofluids*, vol. 10, pp. 1-17, 2021, doi: <https://doi.org/10.1016/j.ijft.2021.100071>.
- [8] E. Novianarenti, E. Ningsih, and N. A. Rahman, "Calculation Study of Double Pipe Type Heat Exchanger in LNG Plant Pre-Design with Capacity 250 tons/hour," *J. Mech. Eng. Sci. Innov.*, vol. 4, no. 1, pp. 27-34, 2024, doi: 10.31284/j.jmesi.2024.v4i1.5164.
- [9] M. El Hassan, A. Y. Al Rajeh, N. Bukharin, et al., "Performance Enhancement of Convective Heat Transfer in Double Pipe Heat Exchangers using Different Vortex Generatorsa-Configurations," in *International Conference on Renewable Energy and Environment Engineering*, Brest, France: EDP Sciences, 2025, pp. 1-9. doi: 10.1051/e3sconf/202564702002.

- [10] M. A. M. Ali, W. M. El-Maghlany, Y. A. Eldrainy, et al., "Heat transfer enhancement of double pipe heat exchanger using rotating of variable eccentricity inner pipe," *Alexandria Eng. J.*, vol. 57, no. 4, pp. 3709-3725, 2018, doi: 10.1016/j.aej.2018.03.003.
- [11] S. A. Al-Rawashdeh, "CFD Analysis of Heat Exchanger Effectiveness and LMTD with Varying Pipe Length," *Emerg. Sci. J.*, vol. 9, no. 4, pp. 2118-2131, 2025, doi: 10.28991/ESJ-2025-09-04-020.
- [12] S. S. M. Ajarostaghi, M. Zaboli, H. Javadi, et al., "A Review of Recent Passive Heat Transfer Enhancement Methods," *Energies*, vol. 15, no. 3, pp. 1-60, 2022, doi: 10.3390/en15030986.
- [13] A. S. B. Wardhani, A. T. Labumay, and E. Ningsih, "Influence of Fluid Inflow Rate on Performance Effectiveness of Shell and Tube Type Heat Exchanger," *J. Mech. Eng. Sci. Innov.*, vol. 2, no. 1, pp. 9-15, 2022, doi: 10.31284/j.jmesi.2022.v2i1.2993.
- [14] E. Tavousi, N. Perera, D. Flynn, et al., "Heat transfer and fluid flow characteristics of the passive method in double tube heat exchangers: A critical review," *Int. J. Thermofluids*, vol. 17, pp. 1-29, 2023, doi: 10.1016/j.ijft.2023.100282.
- [15] Z. S. Kareem, M. N. Mohd Jaafar, T. M. Lazim, et al., "Passive heat transfer enhancement review in corrugation," *Exp. Therm. Fluid Sci.*, vol. 68, pp. 22-38, 2015, doi: 10.1016/j.expthermflusci.2015.04.012.
- [16] Y. Shi, C. Liu, H. Chen, et al., "Impact of Corrugated Fins on Flow and Heat Transfer Performance in Medium-Deep Coaxial Underground Heat Exchangers," *Energies*, vol. 18, no. 9, pp. 1-18, 2025, doi: 10.3390/en18092212.
- [17] J. I. Córcoles, J. D. Moya-Rico, A. E. Molina, et al., "Numerical and experimental study of the heat transfer process in a double pipe heat exchanger with inner corrugated tubes," *Int. J. Therm. Sci.*, vol. 158, pp. 1-21, 2020, doi: 10.1016/j.ijthermalsci.2020.106526.
- [18] P. K. Chaurasiya, J. Heeraman, A. P. Singh, et al., "Numerical exploration of heat transfer and friction factor in corrugated dual-pipe heat exchangers using SiO<sub>2</sub> and CuO nanofluids," *Therm. Sci. Eng. Prog.*, vol. 56, pp. 1-15, 2024, doi: 10.1016/j.tsep.2024.103076.
- [19] S. Zhu, J. Wang, and J. Xie, "Numerical investigation of the heat transfer characteristics of R290 flow boiling in corrugated tubes with different internal corrugated structures," *Mathematics*, vol. 9, no. 22, pp. 1-17, 2021, doi: 10.3390/math9222969.
- [20] S. Yadav and S. K. Sahu, "Heat transfer and friction factor characteristics of annuli formed by the smooth inner tube and corrugated outer tube-An experimental study," *Exp. Heat Transf.*, vol. 33, no. 1, pp. 18-39, 2020, doi: 10.1080/08916152.2019.1569179.
- [21] W. Wang, Y. Zhang, K. S. Lee, et al., "Optimal design of a double pipe heat exchanger based on the outward helically corrugated tube," *Int. J. Heat Mass Transf.*, vol. 135, pp. 706-716, 2019, doi: 10.1016/j.ijheatmasstransfer.2019.01.115.
- [22] I. M. Arsana, T. W. Wibowo, H. N. Sari, et al., "Effect of Concave Corrugated Tube Shape on The Effectiveness of Double Pipe Heat Exchanger," in *International Conference on Engineering, Technology, and Industrial Application (ICETIA)*, Surakarta, Indonesia: EDP Sciences, 2024, pp. 1-6. doi: 10.1051/e3sconf/202451710002.
- [23] F. R. Menter, M. Kuntz, and R. Langtry, "Ten Years of Industrial Experience with the SST Turbulence Model Turbulence heat and mass transfer," in *Turbulence, Heat and Mass Transfer 4*, K. Hanjalić, Y. Nagano, and M. Tummers, Eds., Begell House Inc., 2003, pp. 625-632.
- [24] P. J. Roache, "Perspective: A method for uniform reporting of grid refinement studies," *J. Fluids Eng.*, vol. 116, no. 3, pp. 405-413, 1994, doi: 10.1115/1.2910291.

- [25] F. W. Dittus and L. M. K. Boelter, "Heat transfer in automobile radiators of the tubular type," *Int. Commun. Heat Mass Transf.*, vol. 12, no. 1, pp. 3-22, 1985, doi: 10.1016/0735-1933(85)90003-X.
- [26] V. Gnielinski, "New Equations for Heat and Mass Transfer in Turbulent Pipe and Channel Flow," *Int. Chem. Eng.*, vol. 16, no. 2, pp. 359-368, 1976.
- [27] H. Blasius, "Grenzschichten in Flüssigkeiten mit kleiner Reibung," *Zeitschrift für Math. und Phys.*, vol. 56, pp. 1-37, 1908.
- [28] B. S. Petukhov, "Heat Transfer and Friction in Turbulent Pipe Flow with Variable Physical Properties," *Adv. Heat Transf.*, vol. 6, pp. 503-564, 1970, doi: 10.1016/S0065-2717(08)70153-9.